DOI 10.31256/UKRAS19.9

In process monitoring and control of automated TIG welding processes

James Dobrzanski, Daniel De Becker, Dr Laura Justham, *UKRAS*

***Abstract* - TIG (Tungsten Inert Gas) welding is utilised in industry as a preferred choice due to its high quality, coupled with the ability to control the shape of the weld bead. In any thermal based material processing, in-process control of the melt zone is essential to achieve optimal process conditions. However, due to the harsh environments during the joining process, including high temperatures and plasma emissions, it remains difficult to monitor the process and react to any conditions which may prove detrimental to the desired properties of the joint. In most cases, the input current and/or arc voltage are monitored during the process to guarantee integrity of the finished joint, backed by destructive testing of sample joints to confirm the output. This research develops a closed-loop adaptive control system based on thermal imaging to address the fluctuations observed during the TIG welding process. The experimental setup comprised of a robotic TIG welding system, single wavelength IR (Infrared) thermal camera, a data acquisition system and an NI (National Instruments) based DAQ controller. The results show that the online monitoring and closed loop control of the TIG welding process can help to minimise defects and the proposed system can be readily adapted to any thermal based manufacturing techniques.**

I. INTRODUCTION

Tungsten Inert Gas (TIG) welding is required in applications where a high-quality joint is necessary. However due to the heterogeneous nature of this type of joint there are yield limitations associated with productions of such joints. Typically, within literature, four major variables are synonymous with the creation of high-quality joints; welding current, arc voltage, welding electrode speed across the workpiece, and shielding gas composition [1]. A high level of interdependence between these variables adds further complexity to the process. An increase in electrode speed requires a corresponding increase of current to satisfactorily melt the material to be welded. This subsequently increases both the pressure within the welded joint and the flow of molten material, creating a periodic irregular surface profile of the joint. This leads to defects within the joint, which can affect its integrity [2 - 3].

Thus far, the focus on utilization of infrared thermography (IRT) has been for its use as a monitoring tool. A variety of industries opt to utilize this equipment due to the non-contact non-destructive means of operation. Temperature has been identified as one the most common indicators of structural health of both plant and components, with the ability to monitor a system's condition and therefore health in real-time [4]. Condition monitoring is an in process monitoring technique of plant and procedures. In the case of TIG welding, condition monitoring refers not only to the structure and visual condition of the welded joint but also the equipment behavior during the welding cycle. This may include heat build-up within the welding electrode, heat shield, and gas nozzle; which may help to identify deterioration in equipment before a failure occurs, resulting in both damage to the plant and a compromise to the joint integrity. Previous work on how the introduction of an IRT unit is able to help in a multivariable control system can be used in welding control has been primarily focused on MIG welding processes. With modern process control focusing on the development of laser-based material processing.to understand [5-7]. This work looks to expand the scope of this to TIG welding. TIG welding differs by using a non-consumable electrode which may obscure or influence the ROIs (Region of Interest) of the IRT system. Careful placement of the camera with respect to the melt pool is required to mitigate these effects.

During the welding process, undesirable signals from specular reflection of the hot electrode on a metallic surface or from heat accumulation within the torch heat shield may occur. The use of an IRT (Infrared Thermographic) camera offers greater flexibility than the use of single spot infrared sensor technologies used in the testing processes of Wikle [8} The two-dimensional area monitoring offered by IRT cameras allow for the observation of multiple areas of emission. Whilst masking areas where unwanted signals may occur.

The aim of the work presented in this paper was to develop a robust adaptive control system based on thermography for automated control of the HAZ shape and width in the TIG welding process. Event based control offers a method of filtering the signal response to slow the system's reaction to the current input.

II. EQUIPMENT AND METHODOLOGY

The material chosen for the task was stainless steel 316, with a filler wire of 0.52 mm² CSA (Cross sectional Area) matching the material type. The blanks for welding dimensioned 150 mm x 50 mm x 1.5 mm and a gap spacing of 0.2 mm was used during the welding procedure. This gap allows for some small thermal expansion of the material during the welding operation and is appropriate as the gap should not exceed the diameter of the filler wire, which was 0.8 mm, to ensure the filler wire can successfully bridge the gaps between the parts being welded. A jigging fixture to stop the blanks from moving during the welding process was also used.

The welding power source is a Fronius Magicwave 4000 capable of operating in a fully autonomous mode, receiving its control signals during operation. A Fronius Robacta PTW 1500 torch handle, welding currents up to 150 A (with suitable

J Dobrzanski is with the Intelligent Automation Centre at Loughborough University, LE11 3QZ, UK (email: J.Dobrzanski@lboro.ac.uk).
D De Becker is with the Intelligent Automation Centre at Loughborough University, LE11 3QZ, UK (email: d.de-becker@lboro.ac.uk).
L Justham is with the Intelligent Automation Centre at Loughborough University, LE11 3QZ, UK (email: L.Justham@lboro.ac.uk

shielding nozzle and gas flow) was also used. The electrode used was a 2.6 mm diameter tungsten electrode doped with 2% thorium. The welding torch was attached to the end effector of a KUKA kr16-2 6 axis robot controlled by a KRC2 robot controller. A custom robot program ensured the repeatability of the robot path during the experiments. A national instruments PXI module handled communication to the robot and control signals to the welding unit. Expansion modules allow for the transmission of both analogue and digital signals. An image of the robotic welding setup can be seen in Figure 1. The IRT is place in an isometric chase position to stop the reflection of the Tungsten influencing the recorded temperature of the melt pool.

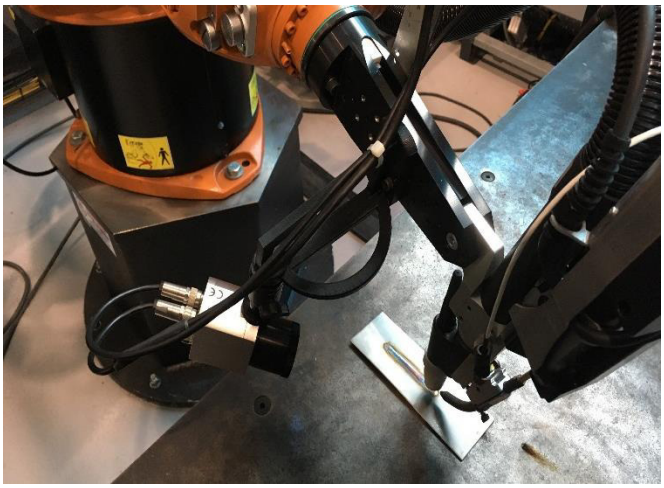

Figure 1. The welding components on the end effector of the robotic arm

A Micro Epsilon thermaIMAGER TIM M1 managed the thermography elements. A 16mm 12 ° field of view (FOV) lens allowed the entire melt pool during the welding process to be captured when coupled with the thermal camera. A custom program offers NI LabVIEW the ability to monitor and control the process during operation. This program used closed loop feedback to facilitate temperature data from the IRT controlling the welding current during operation.

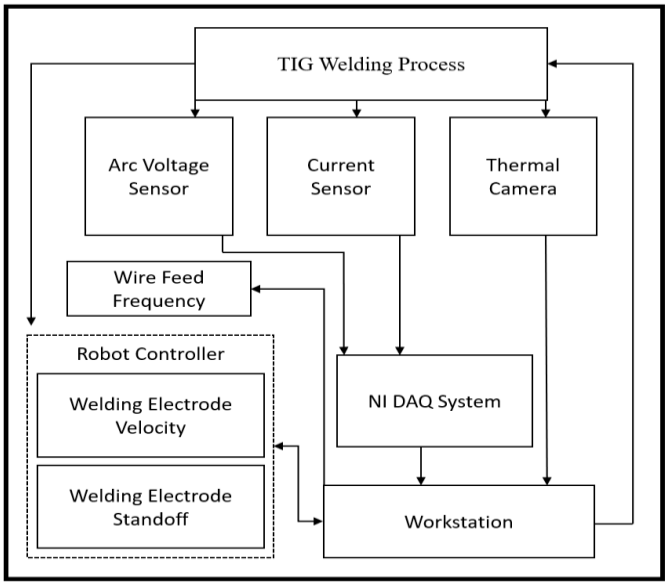

Figure 2 System diagram of the experimental set up

The main components of the developed adaptive control system are shown in Figure 2. The arrows highlight the communication between each of the devices.

D-optimal methodology of experimental design is used with the aid of design expert software; this design allows for the use of pre-defined central core values with incremented and decremented steps from the chosen core values to help identify the true optimal equipment settings and how their interaction affects one another. Interviews of skilled TIG welders provided the initial choices for the number and values of the parameters used as a base for the initial runs of the robotic welding. These settings are in Table 1 row 5.

The TIG welded samples were tested and analysed with two different methods. The first means of testing the welded samples was by performing tensile testing. The Second test involved geometric analysis of the joint. The first test will show if the welded joint's tensile strength is equal to that of the base material. If the joint fails prematurely then we must assume the welded joint to have a lower tensile strength than that of the base material; stainless steel 316l. The machine used for this testing was an Instron 234 tensile testing machine. Firstly, the welded samples were laser cut into an ISO standard size, as shown in Figure 3a, and this cut sample was placed into the centre of the jaws, which are then locked in place around the sample. The load was then increased until fracture occurred on the specimen. The output from the tensile testing machine is in graphical form showing load vs extension. We can expect to see the UTS of either the joint or the material from this graph, which should occur shortly before fracture. The Instron 234 tensile testing machine is an electromechanical tension-testing machine, which is often referred to as a pull testing machine. As well as tension testing these machines are also able to perform shear, peel, tear, cyclic and bend tests. The Instron 234 tensile testing machine is able to perform tensile tests of up to 100kN, at a maximum pull speed of 500mm/min, with a load accuracy of 0.05%, and data acquisition rate of 500Hz.

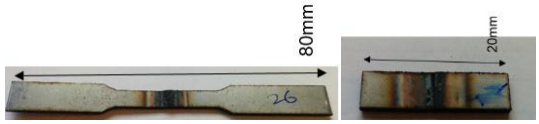

(a) *(b)*

Figure 3. Samples used for (a) mechanical and (b) Geometric analysis

Figure 3b shows a laser cut sample for use in microscopic analysis of the welded joint. The sample is cut from the HAZ (Heat Affected Zone) of the weld, then encased in a resin block. Finally, the edge of the sample was machined upon its edge to remove any processing of the material via the laser cutting process and analysed for imperfections and joint geometry.

III. Results and Discussion

The initial set of experiments were devised to identify the KPVs of TIG welding and the effect of parameters on TIG welding quality. This information was used as a baseline to find the optimal settings for further experimentation related to automation. The primary KPV's selected for analysis were welding current, welding voltage, electrode standoff,

electrode angle, and electrode velocity. Penetration and joint strength were taken as the key output quality parameters Table 1 shows a selection of the parameters used in the welding study.

	Welding Current (A)	Electrode Speed (mm/s)	Electrode Angle (°)	Electrode Standoff (mm)	Wire Feed Rate (mm/s)
Test A	90	5	0	2	2
Test B	50	1	40	5	0
Test C	50	3	0	2	0.5
Test D	50	1	40	2	0
Human Selection	70	3	20	3.5	1

Table 1. Welding parameters

Figure 4 shows the effect of TIG welding parameters on the weld shape and size. Figure 4a shows a high-quality joint with no voids, good penetration and width. Figure 4c shows good penetration but a reduced amount of wire feed during the process has resulted in under filling of the top face of the joint. Low current input to the joint has allowed fusion to occur but has resulted in the formation of voids within the joint. Figure 4b shows a severe lack of material in the joint, this has resulted in a very narrow joint. Figure 4d shows good penetration and depth. Poor fusion has resulted in the formation of an undercut in the joint which would seriously compromise the joint strength.

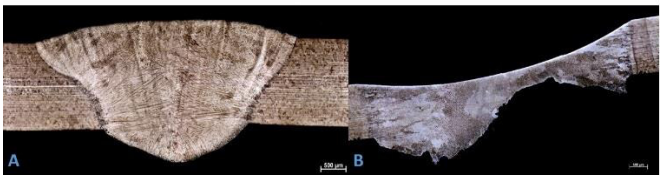

(a) Current=90A; speed=5mm/s ; Electrode angle=0° ;Electrode Standoff = 2mm ;Wire Feed Rate=2mm/s

(b) Current=50A; speed=1mm/s ;Electrode angle=40° ;Electrode Standoff=5mm ; Wire Feed Rate=N/A

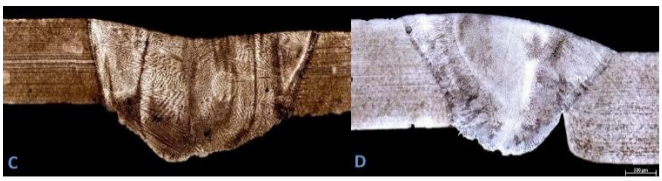

(c) Current=50A; speed=3mm/s ;Electrode angle=0° ;Electrode Standoff=2mm ; Wire Feed Rate=0.5mm/s

(d) Current=50A; speed=1mm/s ;Electrode angle=40° ;Electrode Standoff=2mm ;Wire Feed Rate=N/A

Figure 4. Cross-sectional view of the TIG welded samples

Figure 5 shows a force vs extension graph for each of the four samples tested within the experiment where a cohesive joint was formed. From these results, the following setting as a baseline for the control inputs were determined: Current=90A; Electrode speed=5 mm/s; Electrode angle=0 °; Electrode Standoff=2 mm; Wire Feed Rate=2 mm/s. These settings produced the strongest, most ductile weld. Stainless Steel 316l has a Solidus temperature of 1375 °C, with the material becoming liquid at a temperature of approximately 1400 °C. A weld is unable to be formed until the material of the 2 halves to be joined are molten and have mixed to form one cohesive joint. Due to this, a temperature of 1450 °C was selected as the initial target temperature for the melt pool. This was then set as the control point for the system to maintain during operation to control the width of the HAZ

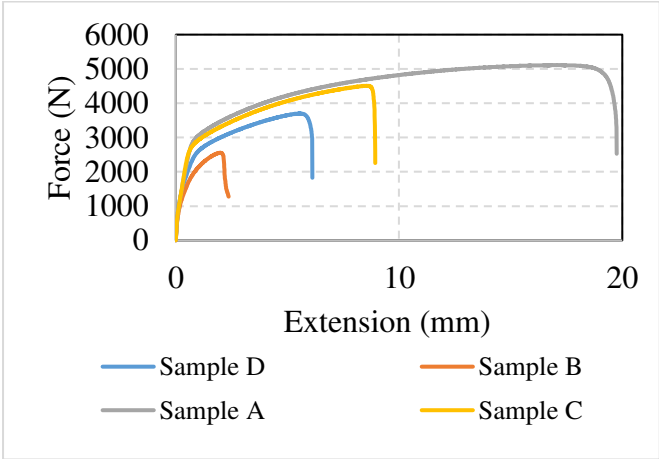

Figure 5. Force vs Extension on for various TIG welded samples ((a)90 A; 5 mm/s; 0°; 2 mm; 2 mm/s; (b) 50 A; 1 mm/s; 40°; 5 mm; 0 mm/s; (c) 50 A; 3 mm/s; 0°; 2 mm; 0.5 mm/s;(d)50 A; 1 mm/s; 40°; 2 mm; 0 mm/s)

With the optimal parameters established for the welding of 316l with the equipment; optimization of the HAZ was undertaken using thermography as a control input. Images from the adaptive control system can be observed from Figure 6. The aim of the control system was to maintain a melt pool temperature of 1450 °C. Figure 6a shows an initial condition of 1440 °C, this is too low and the current input into the joint is raised (and therefore also the power input). The result is the temperature in 6B of 1459 °C. The control system recognizes this as having excess heat within the joint and therefore reduces the input current. The reaction time to each of the changes in power input is 100 ms, with the current step change of 0,1 A.

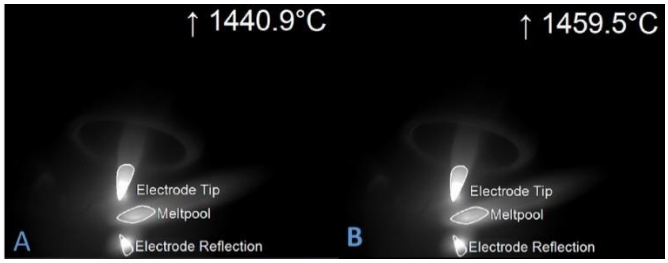

Figure 6. Image (A-B) showing the measurement phase of the melt pool temperature

To determine the benefits 2D thermography for control rather than just condition monitoring, visual analysis of the welded samples was undertaken. Images of the welded samples can be viewed in Figure 7, with blob analysis coupled with Matlab functions created to apply a best-fit line to the edges of the HAZ boundaries and the deviation from it measured in mm from the boundaries. Table 1 shows that thermographic control helps to establish a HAZ with greater uniformity with closed loop control vs the open loop system. The mean error of the HAZ boundary has decreased from 0.18 to 0.14mm on the upper boundary, an improvement of 22%. The lower boundary shows a greater improvement in linearity with an improvement from 0.21mm to 0.12mm, just over 82%. Whilst also controlling the shape of the HAZ, the width can also determine how stresses concentrate around a joint to help identify potential weaknesses in the joint. Ideally the width of the joint will be as narrow as possible with only the edges of the joint affected by the joining process. The average width of the HAZ showed a decrease in width of 5%. Typically, to reduce the width of the HAZ, welding at increased current coupled with increased electrode speed across the melt pool is required. The benefit of a HAZ is the subsequent reduction in residual stresses internal to the welded joint. Therefore, control over the current has also allowed for greater uniformity of the HAZ boundary with a significant improvement in the standard deviation observed.

	Mean Error of upper HAZ	**Mean Error of Lower HAZ**	**Average HAZ Width (mm)**	**S.D. (δ) of Upper HAZ**	**S.D. (δ) of Lower HAZ**
Without Control	0.18	0.21	10.67	0.22	0.26
With Control	0.14	0.12	10.14	0.06	0.05
Improvement	22.28 %	82.20 %	5.19%	0.16	0.21

Table 2. Results

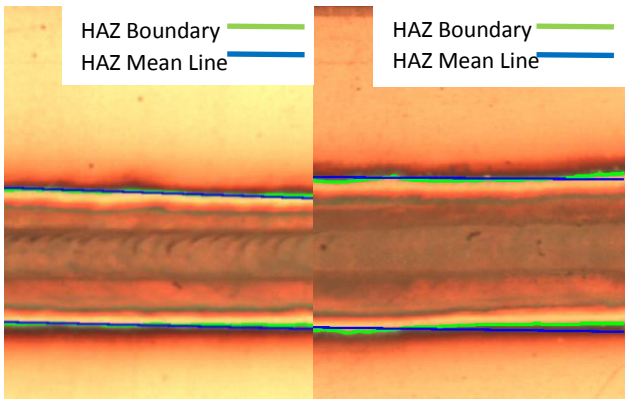

Figure 7. The welded samples

IV. CONCLUSION

Traditional methods of closed loop control for welding systems rely on sending a control signal to the power source reading the current supplied by the primary side of the transformer to control the welding current. The system developed and presented here aims to compliment this with the addition of a weld pool monitoring system which can send a control signal to the power source to modify the welding current and maintain the melt pool temperature for optimal joining conditions. The output from the system utilizing an event based thermographic control shows improvement over the open loop system. The introduction of signal feedback allows for finer control of the HAZ shape than offered simply via the power source alone. In addition, the system is able to react to heat build-up within the material caused by the welding process and impurities within the material creating hot spots in the joint. Further study into the use of more advanced control techniques using PID (Proportional, Integral, Differential) control and image processing techniques coupled with machine learning hope to offer decreased response times of the system and further control of the HAZ.

ACKNOWLEDGEMENTS

This research was carried out with the help of funding from the EPSRC. The authors would also like to IA-CIM for the use of equipment and lab space to conduct these experiments.

REFERENCES

[1] Pires, J.N., Loureiro, A., Bölmsjo, G., 2006. Welding Technology In: Welding Robots: Technology, System Issues and Applications. Springer Science Business Media, Germany, pp. 31–34.

[2] Zhao, C.X., Steijn, V.van, Richardson, I.M., Kleijn, C.R., Kenjeres, S., Saldi, Z., 2009. Unsteady interfacial phenomena during inward weld pool flow with an active surface oxide. Sci. Technol. Weld. Join. 14 (2), 132–140

[3] Lin, M.L., Eagar, E.T.W., 2005. Influence of Surface Depression and Convection on Arc Weld Pool Geometry, vol. 10. Transport Phenomena in Materials Processing, USA, pp. 63–69.

[4] Bagavathiappan, S., Lahiri, B.B., Saravanan, T., Philip, J. and Jayakumar, T., 2013. Infrared thermography for condition monitoring–a review. Infrared Physics & Technology, 60, pp.35-55.

[5] C. C. Doumanidis and David E. Hardt, 1988. Multivariable Adaptive Control of Thermal Properties During Welding: Journal of Dynamic Systems, Measurement, and Control 113, pp. 22-92.

[6] Mansoor A. Khan, Nels H. Madsen, Nels H. Madsen, John S. Goodling, John S. Goodling, Bryan A. Chin, Bryan A. Chin, "Infrared Thermography As A Control For The Welding Process," Optical Engineering 25(6), 256799 (1 June 1986). , 113, pp.228-233.

[7] Gade, R. & Moeslund, T.B. Thermal cameras and applications: a survey: Machine Vision and Applications (2014) 25: 245. https://doi.org/10.1007/s00138-013-0570-5

[8] H.C Wikle S.Kottilingam, R.H Zee, B.A Chin., 2011. Infrared sensing techniques for penetration depth control of the submerged arc welding process, 113, pp.228-233.